Analysis and validation of integral pool spreading model of LNG spills on concrete

Nisa Ulumuddin, Tomasz Olewski*, and Luc Véchot

Mary Kay O'Connor Process Safety Center - Qatar

Texas A&M University at Qatar, PO Box 23874, Education City, Doha, Qatar

*Corresponding author: tomasz.olewski@qatar.tamu.edu

When a loss of primary containment of liquefied natural gas (LNG) occurs on the ground, a pool, that simultaneously spreads and vaporizes, is formed posing cryogenic, asphyxiating, and flammable hazards to its surrounding. Determining the pool size and vapour generation upon release play key roles in the accuracy of dispersion and consequence models. This work focuses on LNG source term model validation through the evaluation of an existing model with a newly generated data.

A field-scale experimental setup was designed to study the pool temperature, pool spreading and heat flux from the concrete following a release of cryogenic liquid. In this work, liquid nitrogen (LIN) was used as a safer analogue to LNG as it is a non-toxic non-flammable cryogen. The experiments were carried out inside a 6×5×1.2 m (width x length x depth) pit.

The Gas Accumulation over a Spreading Pool (GASP) model was implemented and used to predict the vaporization and pool spreading rates of the experiment and a spill from selected literature. The model assumes that the pool boils until it completely vaporizes, meaning that there is no switch to the evaporation regime, which is consistent with obtained experimental results. The pool radius estimated by GASP was found to be relatively close with the experimental data, but it did not simulate the pool growth as consistently as the simulation with Moorhouse and Carpenter (1986) data. Vaporization inside the discharge hose was speculated to have decreased the discharge rate of LIN onto the ground, causing the pool to spread slower at the beginning of the spill and thus not match the input data to the model. It is also possible that the model does not simulate slow spills well, as reproduced by the GASP simulations of Nguyen *et al.* (2015)'s LIN spill. The accuracy of Fourier's one-dimensional conduction equation for modelling conduction through the concrete was also tested by comparing the predicted temperature with experimental temperature. The study showed that the model is sufficient to predict heat transfer inside the concrete as long as the substrate thermal properties change as a function of temperature.

Keywords: Cryogenic liquid spill, liquid nitrogen, pool spreading, source term modelling.

Introduction

Global demands for cleaner abundant energy are one of the drivers of the natural gas industry. The total liquefied natural gas (LNG) trade is still a growing number, reaching 258M metric tonnes in 2016, which was a 13.1 M metric tons increase from the previous year. Qatar remains as the largest LNG exporter, with an export of 77.2 M metric tons, approximately a third of the global LNG supply (International Gas Union, 2017).

LNG has specific characteristics that create challenges for the safety of LNG production, transport, and storage. It poses flammable, cryogenic, and asphyxiation hazards to its surrounding. In the particular scenario of a spill of LNG on ground, a liquid pool forms, simultaneously spreading and vaporizing at a rate proportional to the heat received from the surroundings. The generated vapour forms a dense cloud that moves downwind and may ignite if the cloud is within its flammability limit of 4.4 to 17 vol./vol. % given that enough ignition energy is provided.

Modelling LNG spills on the ground requires coupling the pool spreading model with heat transfer models. Most conductive heat transfer models have been based on Fourier's one-dimensional heat conduction equation, and they contain assumptions which may not reflect reality as LNG is boiling. The first most common simplification is the boundary conditions of the conduction heat transfer; the ground surface is set to the liquid boiling temperature when in contact with the liquid, and is set to ambient temperature outside of the pool. In reality, the temperature of the ground not in direct contact with the liquid may still be cooler than the ambient temperature. Most vaporization models also assume perfect thermal contact between the ground and the liquid, which is not realistic because of the bubbles formed during boiling. Whether these models are sufficient for the modelling of LNG releases depend on the outcome of its validation checks to be done in this paper.

When spilled on the ground, LNG will form a liquid pool spreading on the surface. As the surface area of the pool is growing, the overall vaporization rate increases. The rate at which the pool spreads depends on the forces acting on the liquid pool as described by the three following pool spreading regimes, the gravity-inertia, gravity-viscous, and surface tension-viscous regimes.

The "Gravity-Inertia Regime" occurs when the main driving force of the pool spread is gravity and the resisting force to the spread is the liquid inertia. This regime is expected at early stage of the pool development, just after the release. The downward gravitational force acting on the pool causes an uneven pressure distribution within the pool, causing the pool to spread sideways. With time, the pool becomes thinner and thus the gravity force decreases, and the pool spreading decelerates. The inertia of the moving liquid restricts the pool spreading. As the pool develops and immediately covers larger surface area, the effect of the liquid inertia diminishes and viscous friction generated between the pool and the ground becomes the dominant

resistance to the pool spread. If the pool becomes very shallow, the effect of gravity becomes infinitesimal. The surface tension between the liquid-surface interfaces becomes the prevailing pool driving force. For a cryogenic spill on land, the surface tension-viscous regime may perhaps only be reached on smooth surfaces and have not been experimentally achieved. For a spill on normal rough surfaces, it is more likely for the pool to completely vaporize before the surface-tension force becomes dominant (Webber et al., 2010). In summary, pool spreading is governed by the dominant driving and resisting forces.

There are several programs built commercially for cryogenic releases. Of these include Gas Accumulation over a Spreading Pool (GASP), LPOOL, SOURCE5, Liquid Spill Modeling System (LSMS), Process Hazard Analysis Software Tool (PVAP), and SuperChems™. All of these models consist of a pool spreading model and a vaporization model. Although the basis of the models used in these programs are all similar, their accuracies vary. For instance, while the conductive heat transfer models in most programs are based on Fourier's ideal conduction equation, different programs solved the equations differently. PVAP and SOURCE5 assumes that conductive heat transfer is uniform across the pool while GASP, LPOOL, and SuperChems™ takes into account pool contact with warmer ground during the spreading of the pool. Secondly, all of the pool spreading models incorporated are based on the partial differential shallow-water equations. However, while some models such as LPOOL, LSMS and SuperChem™ solves the set of equations numerically, others such as SOURCE5, PVAP and GASP made simplifications to the equations which makes it easier and faster to compute.

There is a lack of experimental data available for cryogenic spills on concrete. Data provided by Reid and Wang (1978), Lang *et al.* (1980), Vechot *et al.* (2017), and Quraishy *et al.* (2015) consist of liquid nitrogen vaporization rates at lab-scale, where vaporization is measured for a non-spreading pool. Such data provides an incomplete result for LNG spill model validation, as the pool is not in contact with new ground and the total heat flux into the pool decreased as the ground cools down. In a real case or an accident, LNG is typically spilled over a large or unbounded area, meaning that the pool edge is in contact with new warmer ground at all of the time. Data of a vaporizing spreading pool will thus give better insight to the accuracy of LNG source term model predictions. Experiments which take into account pool spreading have been generated by Moorhouse and Carpenter (1986). However, compared to vaporization experiments, little information regarding the substrate were provided. To improve the validation of existing source term models, additional experimental data observing cryogenic pool spreading are needed.

This research was comprised of two components:

- Modelling part: An existing integral vaporizing pool spreading model was implemented using MATLAB. Prior to its use, the code was verified and validated with existing literature data.
- Experimental part: Two liquid nitrogen spills inside a large concrete pit was conducted, recording pool radius and concrete temperature, release conditions and the weather data required for model validation.

Liquid nitrogen was used as a safer analogue to LNG as it is a non-flammable cryogen. This project aims to bring insight to the validity of common conduction and pool spreading models when LNG is spilled onto the ground. The scope of this work includes the validation work of a well-recognized vaporizing pool spreading model with the experimental data.

Methodology

Description of Model

A widely accepted source term model in literature was implemented in order to simulate pool spreading and conduction. Gas Accumulation and Spreading Pools (GASP) is one of the few models in which its algorithm and derivations have been published in-depth (Webber et al. 2010; Webber, 1991; Webber and Brighton, 1987) It has been used by a number of organizations including Health and Safety Environment (HSE), UK Atomic Energy Authority (UKAEA), AEA Technology, ESR Technology, BP, TNO and many others, proving its usability (Webber et al., 2010). The GASP model has been validated with Reid and Wang (1978)'s LNG spills on insulating concrete and Hankinson and Murphy (1987)'s butane experiments on insulating floor to validate the vaporization model (Webber et al., 2010). To validate for the simultaneous spreading and vaporization, so far, GASP was plotted against the LNG radius profile generated by Moorhouse and Carpenter (1986) and found good agreement (Webber et al., 2010).

The model simultaneously solves ordinary differential equations of mass, radius, and velocity, and an integral equation of conductive heat transfer. Other modes of heat transfer were neglected in this model as their contribution within the validation exercises conducted in this paper were minimal. The model was implemented and solved using MATLAB version R2016b. The MATLAB algorithm and solution were also verified by implementing the same equations into Polymath. It was then validated with existing experimental data available on literature. A limiting factor of GASP tolerated in this study is that it does not consider phase change before the liquid reaches the ground. Phase change before the liquid touches the ground is not taken into account in GASP.

Equation 1 and Equation 2 display the set of pool spreading equations for instantaneous and continuous spills on land.

$$\frac{dr}{dt} = U \qquad \text{Equation 1}$$

$$\frac{dU}{dt} = \frac{4g(1-s)h}{r} - F \qquad \text{Equation 2}$$

Where *r* is radius, *F* is the effect of friction over the bottom area of the pool, *U* is velocity, and *s* is the shape factor which is assumed 0 for a smooth ground.

The acceleration of the pool spread is described in Equation 2, where it is the resultant of the resisting and driving forces. The friction term consists of the summation of the turbulent and laminar terms shown in Equation 3. They depend on the velocity which in turn is dependent on the radius of the pool. The dimensionless constants C_{Lam} and C_{Turb} are provided by Webber (1991) and Webber and Brighton, (1987).

$$F_{Lam} = C_{Lam}\frac{vU}{h^2} \qquad F_{Turb} = C_{Turb}\frac{U^2}{h} \qquad \text{Equation 3}$$

Where *v* is kinetic viscosity and *C* is an empirical constant.

The depth *h* is calculated as the volume of pool divided by its area.

For continuous spills, a mass balance shown in Equation 4 is necessary.

$$\frac{dV}{dt} = S - Vap \qquad \text{Equation 4}$$

Where *S* is the spill rate and *Vap* is the vaporization term. To model spills into a bund, the maximum radius of the pool is restricted by the bund dimensions and its spreading rate becomes 0.

GASP's solution to Fourier's conduction equation is shown in Equation 5.

$$Q_l(t) = -\frac{k\phi(t)}{\sqrt{\pi\alpha t}} - \frac{k}{A(t)\sqrt{4\pi a}}\int_0^t dt'(t-t')^{-\frac{3}{2}}[\phi(t)A(t) - \phi(t')A(t')] \qquad \text{Equation 5}$$

$$\phi(t) = T(t) - T_a \qquad \text{Equation 6}$$

$$A(t) = \pi r^2(t) \qquad \text{Equation 7}$$

The conduction heat transfer model in GASP assumes that the ground is semi-infinite and is initially at ambient temperature. For a cryogenic spill, the ground is set to the boiling temperature as soon as they are in contact. The first term consists of the ideal heat flux equation at the centre of the pool. The second term in Equation 5 allows for the fact that the outer rings of the pool are in contact with new warm ground, and thus heat transfer decreases towards the centre of the pool. When the pool reaches the borders of the bund, the second term in Equation 5 becomes 0 as the area difference becomes naught. There are no additional equations for different boiling regimes and thermal contact between the pool and the grounds is assumed perfect, which are not true in reality due to bubble formation during boiling.

Experimental Setup

A medium-scale field experiment has been performed utilizing liquid nitrogen as a safer analogue of LNG to provide data useful for models validation. The liquid nitrogen is a cryogenic liquid and thus the generated experimental data may be valuable for validation of LNG source term models. In addition, conducting large spills of liquid nitrogen allows for the learning curve of experimenting with LNG in the future. The experiment was conducted at the LNG facility at Ras Laffan Emergency and Safety College in Doha, Qatar.

The experiment was conducted in two trials on separate days. A total of approximately 10,000 litres of liquid nitrogen were spilled in each trial into a concrete pit of size 5 × 6 × 1.2 m (length x width x height) through a 15 m long cryogenic hose, which was attached to wooden frame and hose nozzle was positioned in the centre of the pit (Figure 2a). Properties of the concrete substrate have been characterized during the construction of the facility. Rounded values for thermal conductivity and diffusivity are given in Table 1 when its temperature is 25°C. The concrete composition is given in Table 2. The thermal conductivity and diffusivity values for this concrete for wider range of temperatures, from -160 to 50°C, were published earlier by Ahammad *et al.* (2017).

Table 1: Concrete physical and thermal properties

Thermal conductivity, W m^{-1} K^{-1}	**1.13**
Specific heat, J g^{-1} K^{-1}	0.92
Thermal diffusivity, m^2 s^{-1}	5.29 × 10^{-7}
Average density, kg m^{-3}	2323 ± 70
Average surface roughness, mm	17.0 ± 7.3

Table 2: Concrete composition

Component	Part by weight
Aggregate (20 and 10 mm recrystallized limestone; 20/10mm ratio is 1.5 weight/weight)	3
Washed Sand	2
Dry Portland Cement	1

The concrete pit was instrumented with thermocouples (XCIB-N-3 by OMEGA Engineering), which were distributed at the surface of the pit base to measure the pool spreading (Figure 1). The liquid was detected at the certain location when the thermocouple reading displayed a value close to the boiling point of liquid nitrogen (approximately -196◦C). Thermocouples were attached to a wooden structure, installed at around 10 cm above the base surface, for a fixed location of each thermocouple (Figure 2a). The pit sides were labelled as facility north (not true north), west, east, and south, and an 8-direction radial coordinate system (N, S, E, W, NE, SE, SW, SE) was used to indicate the thermocouples locations on the surface. Along each line, the thermocouples were approximately spaced 1 m apart as shown in Figure 1. The north of the pit (facility north) is 20° east to the geographical true north. The pit has a 1% slope from the highest NE corner towards the SW corner, where a small sump was constructed.

The whole pit was surrounded by 1.2 m tall wooden fences with the purpose of minimizing the effects of wind towards the pool (Figure 2a**Error! Reference source not found.**). Oxygen gas detectors were positioned around the pit and near the tanker to monitor oxygen deficient atmosphere outside of the pit to ensure the safety of personnel during the experiment (Figure 2b**Error! Reference source not found.**). The tanker was located around 12 m away from the pit while the control room was located 80 m away (Figure 3).

A total of 100 thermocouples and 13 heat flux plates were embedded in the concrete of the base and walls of the pit to measure the heat transfer and temperature inside the substrate (shown in Figure 4). The sensors embedded inside the pit base were located within a 3 x 3 grid at two vertical layers, 0.05 and 0.15 m below the surface. In total, there were 18 nodes (locations) under the base. Redundant sensors were installed at each node to increase the reliability of each reading, which gives 36 temperature measurements inside the pit base. The rest were installed inside the walls. All the sensors were connected to either the north or east marshalling panel and digital signals were received at the control room (Figure 3).

In both trials, the discharge hose nozzle was installed at a height of 15 cm above the ground and was pointed downward so that the spill impinged on the ground. Both trials were conducted when the atmospheric stability was either A or C when the air temperature was between 22 – 25 ° C. The wind speed was higher during Trial 1 as it was 6.17 ± 1.25 m s^{-1} in contrast to 1.23 ± 0.77 m s^{-1} during Trial 2. The difference in the solar radiation between Trial 1 and 2 was small, as they were 0.72 ± 0.07 kW m^{-2} and 0.52 ± 0.06 kW m^{-2}. The humidity of the air on both days were also close at 49.1 ± 1.3 % and 50 ± 5.7 % respectively. Table 3 to Table 5 contain a summary of the release and atmospheric conditions measured during the experiment.

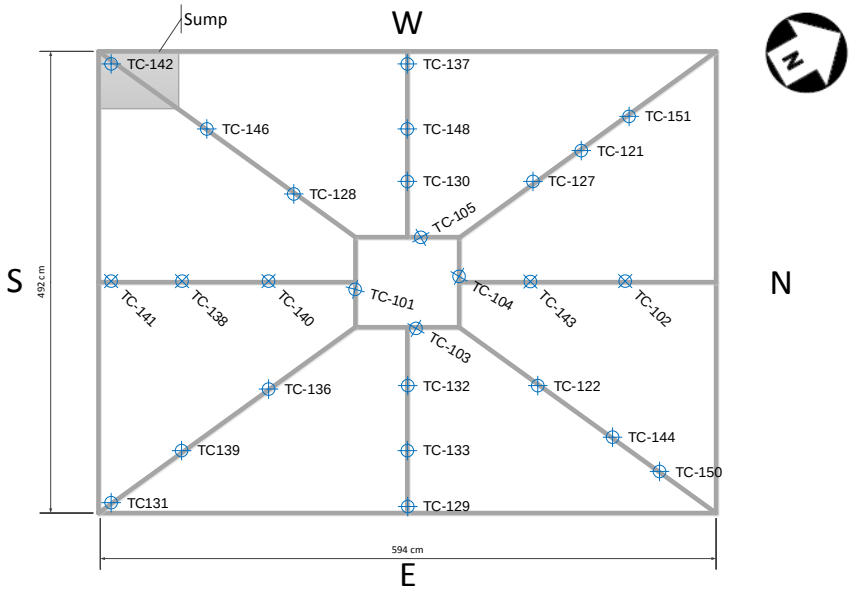

Figure 1: Radius thermocouple arrangement on the pit surface

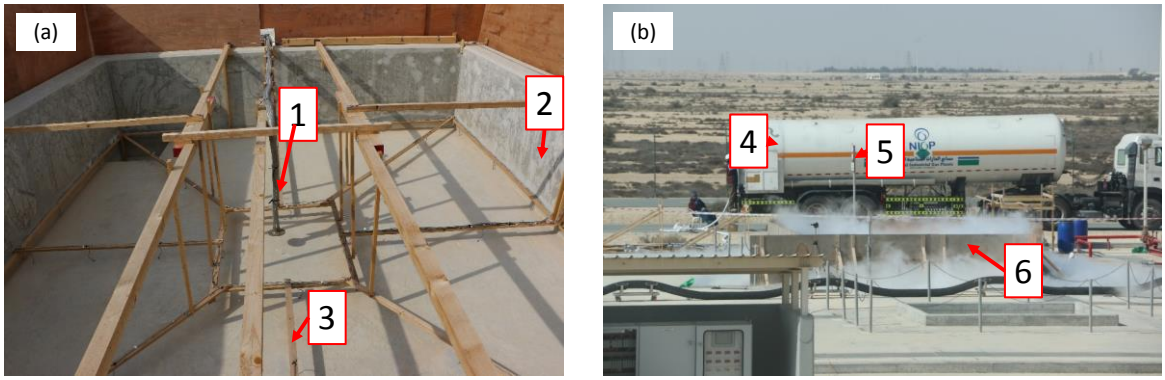

Top and side view of experimental setup:

[1] Delivery cryogenic hose
[2] Thermocouple grid
[3] Concrete pit
[4] Liquid nitrogen tanker
[5] Oxygen gas detector
[6] Wooden fences

Figure 2: Photos of the experiment: (a) wooden structures to support discharge hose and thermocouples; (b) experimental arrangement including location of the road tanker

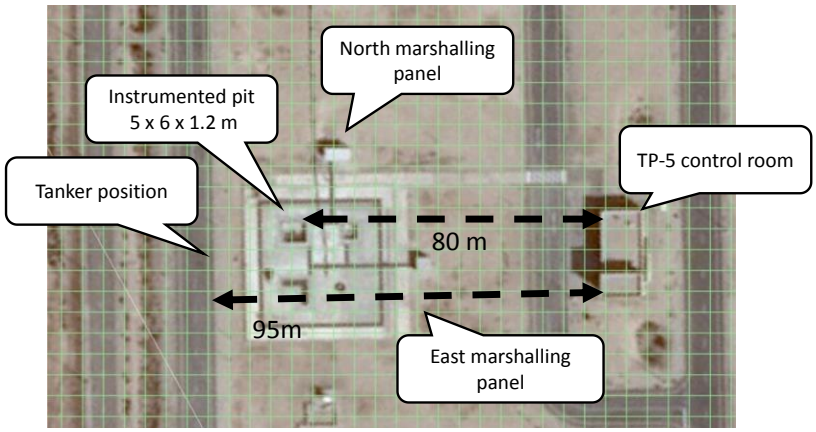

Figure 3: Bird-eye view of TP-5

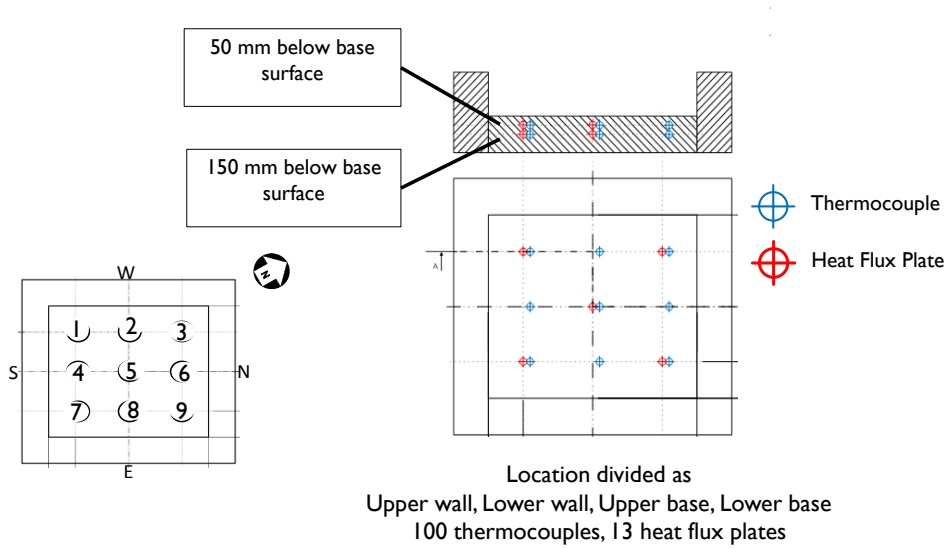

Figure 4: Schematic diagram of sensors embedded within the base of the concrete

Table 3: Release condition of liquid nitrogen

Release data	Trial 1	Trial 2
Spilled volume, m^3	10.59	11.36
Pressure of tanker, bar	2	4
Density of LN_2, kg m^{-3}	800	800
Release height, cm	15	15

Table 4: Weather conditions

Atmospheric condition	Trial 1	Trial 2
Wind speed @ 2 m, m s^{-1}	6.2 ± 1.3	1.2 ± 0.8
Wind speed @ 10m, m s^{-1}	3.6 ± 1.2	1.8 ± 0.9
Air temperature @ 2m, ^{o} C	24.6 ± 0.5	22.9 ± 1.2
Solar radiation kW m^{-2}	0.72 ± 0.07	0.52 ± 0.06
Humidity, %	49.1 ± 1.3	50 ± 5.7
Atmospheric stability	C	A

The experiment consisted of two trials (two days) of spill into the pit. Two level meters consisting of two vertical series of thermocouples were installed as an attempt to measure vaporization from pool depth change. In both trials, the pool was maintained at depths below the highest level meter thermocouple while managing not to dry out the pit, so the concrete surface is always covered by liquid nitrogen. For this purpose, the spill has to be stopped at the certain times when the level was high, and restored when the liquid level dropped. The action resulted to several spills at each trial, namely two spills for Trial 1 (Spill 1 and 2) and four spills for Trial 2 (Spill 3, 4, 5, and 6).

Readings of the liquid level inside the tanker were taken manually every few minutes until the tanker was empty, which provides the mass change in the tanker and then in turn used to calculate discharge rate, shown in Figure 5 and Figure 6 for Trial 1 and 2 respectively. During the first day (Trial 1), the tanker was kept at a pressure of 2 barg and the liquid nitrogen discharge rate was maintained at approximately 1.5 kg s^{-1} for entire day (Figure 5). During Trial 2, the tanker pressure was higher (around 4 barg) and the discharge flowrate varied from spill to spill within the range of 1.3 and 2.2 kg s^{-1}, possibly due to the flashing of liquid nitrogen caused by high pressure. These observed discharge flowrates were found to be lower than the theoretical flowrate of the spill simulated through PHAST, which was simulated to be 4.38 kg s^{-1} and 6.1 kg s^{-1} respectively. It is speculated that the flowrates were slower because of long 15 m hose and potential for two-phase flow. The summary of the discharge rates is displayed in Table 5.

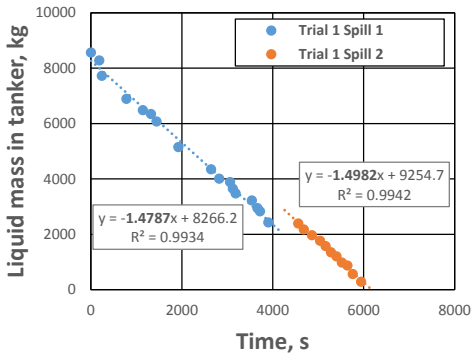

Figure 5: Gradient of spill throughout Trial 1

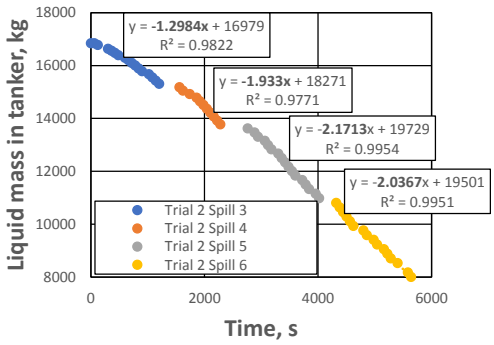

Figure 6: Gradient of spill throughout Trial 2

Table 5: Summary of discharge flowrate of LN_2 in both trials

Trial number	Tanker Pressure	Theoretical flowrate, kg s^{-1}	Observed flowrate, kg s^{-1}
1	2 bar	4.38	1.5
2	4 bar	6.1	1.3, 1.9, 2.2 and 2.0

Uncertainty of Experimental Data

All variables of interest in this experiment: the pool temperature, concrete temperature, and the pool radius indicated by the thermocouples, are associated with two sources of error, a data acquisition error and the inherent error within the sensors. According to the calibration process, the thermocouples embedded in the concrete have an average standard deviation of 0.33° C (accuracy of 0.47%) and a maximum difference of 1.85° C. For thermocouples measuring pool temperature and radius, the average standard deviation of all thermocouples during the calibration process were 0.61° C (accuracy of 1.12%). The positioning of each thermocouple have an uncertainty of ± 2mm as the distance was measured using a meter stick. Detecting when liquid was present at the thermocouple was indicated by a fast temperature drop followed by a flat line below – 196 ° C. In most cases, the cut-off between the vapour and liquid phases are clear. Thus, for the measurement of the pool radius, the uncertainty within the selection of the point when the pool arrived at the thermocouple is ± 3 seconds. Additionally, the responsivity of the sensor to temperature change is 50 ms min floating point (temperature).

Experimental Results and Analysis

Temperature of the liquid pool

There is a need to ensure whether cryogenic spills ever go into evaporative cooling after a release on the ground, or it boils until it completely vaporizes. This can be determined by the measurements of the pool temperature. Two successful trials were performed on separate days. The first trial occurred while the wind speed averaged at 3.7 m s^{-1} ± 1.2 m s^{-1}. The second trial was run when wind speed was at 2 m s^{-1} ± 1 m s^{-1}. While thermocouples installed at the base surface of the pit are reached by liquid they start indicating the liquid nitrogen temperature throughout the experiment. During Trial 1, the thermocouples displayed the boiling temperature of liquid nitrogen after the pool has formed and its temperature does not drop. In the case of Trial 2, the spilled liquid had a temperature lower than the boiling point after which it slowly rose to the boiling point. Temperature drop was also not observed in Trial 2 (Figure 7). Thus, no evaporative cooling was observed during the experiment. This result confirms the lab-scale results obtained by Vechot et al. (2017).

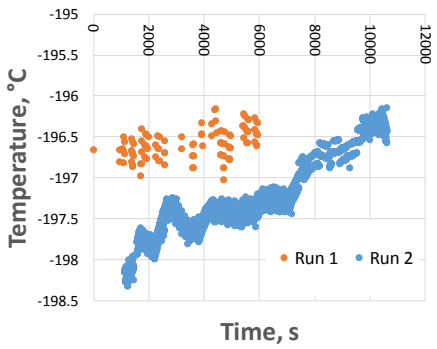

Figure 7: Evidence of boiling during the experiment

Temperature inside the concrete and validation of 1D conduction model

Temperatures inside the concrete were monitored across the base. The nodes where thermocouples are positioned are displayed in Figure 4, where Node 5 is beneath the pool centre. At a depth of 0.05 m inside the concrete, temperature change at the centre of the base was experimentally detected 266 s after the spill (Figure 8). It continues to drop until the end of the experiment. At the outer nodes (Nodes 1, 4, 7), temperature started to have noticeable change after 734 s, after which they eventually reach a minimum temperature of -140 to -146° C. The longer the concrete was exposed to liquid nitrogen, the lower its temperature, reflecting that more heat has been transferred. Lower ground temperature in turn results to a lower heat transfer rate. Therefore, the spreading of the pool directly affects the heat transfer profile across the concrete, where the comparatively lowest heat transfer rate is towards the centre of the pool. This effect was not apparent at 0.15 m under the concrete, as seen in Figure 9.

The 1D conduction model, which is also utilized by GASP, was used to simulate temperature inside concrete at 0.05 m and 0.15 m depths beneath the centre of the pool. A comparison of the simulated and observed concrete temperature was done, shown in Figure 8 and Figure 9. Compared to Node 5 (centre of the base), the simulation indicates that the model is able to predict its temperature exactly for the first 700 s before it progresses to predict a higher concrete temperature during the rest of the pool life.

Table 6: GASP input data for the modelling of experiment at RLESC (Trial 1)

Input data from experiment (Trial 1)	
Liquid	Liquid Nitrogen
Spill rate, kg s^{-1}	1.5
Spill time, s	6720
Initial ground temperature, °C	26.5
Thermal conductivity, W m^{-1} K^{-1}	(see Table 1)
Thermal diffusivity, m^2 s^{-1}	(see Table 1)
Additional assumptions	
Initial h/r ratio (shape of cylindrical tank)	1.5
Ground	Smooth concrete

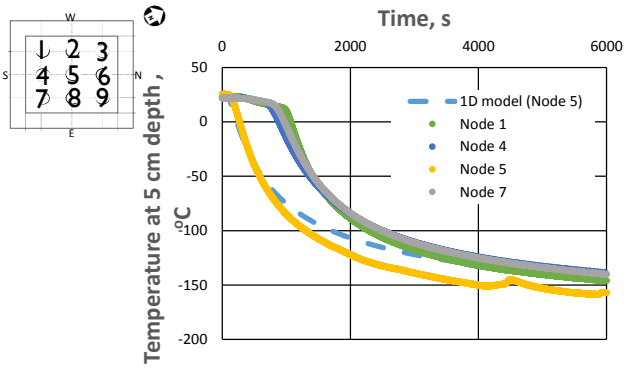

Figure 8: Temperature across the nodes at 0.05 m concrete depth (Trial 1)

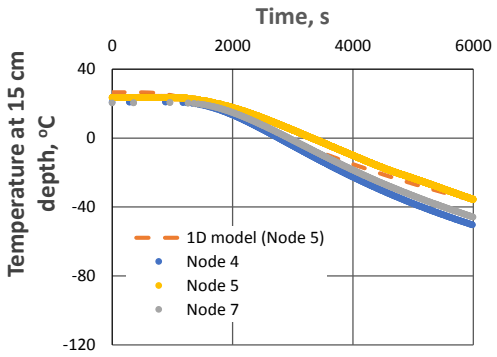

Figure 9: Temperature across the nodes at 0.15 m concrete depth (Trial 1)

During Trial 1, the minimum temperatures inside the concrete at the northern side of the pit was much higher than the southern side. It is due to fact that liquid nitrogen did not reach at Nodes 2, 3, 6 and 9. These observations were supported by the on-surface thermocouple readings as they displayed fluctuating and temperatures much higher than the boiling point, portraying that the nitrogen phase was vapour. These data have been omitted from the graphs. The causes to the non-uniform spread is likely due to the combination of slow liquid nitrogen discharge rate and the sloping of the surface towards the southwest corner. This was later slightly improved in the setup of Trial 2 by increasing the liquid nitrogen spill flowrate. The sloping of the ground, however, would not affect the conclusions regarding heat transfer difference between the centre of the pool (Node 5) and its outer rings (i.e. Nodes 1, 4, and 7).

The effect of the temperature at which the substrate thermal properties was taken at was tested by comparing temperature predictions at 0.05 m and 0.15 m depths using different conductivity values. In **Error! Reference source not found.** and **Error! Reference source not found.**, the concrete temperature is indicated by the blue points. Given the substrate thermal properties as a function of temperature, the conduction model was solved in two conditions; the first condition assumes thermal properties of the ground at ambient temperature, and the second assumes it at the boiling temperature of liquid nitrogen. It was found that nearer to the surface, the model is fitted better when the substrate thermal properties are taken to be the boiling temperature of liquid nitrogen (**Error! Reference source not found.**). Meanwhile, the experimental data at 0.15 m is closer to the model prediction when ambient substrate thermal properties were assumed (**Error! Reference source not found.**). Thus, in order to model the temperature profile inside the concrete, the one-dimensional conduction equation has to be corrected so that the thermal properties of the concrete is dependent on temperature (and not a constant value). There is still a maximum of 11.3% overestimation calculated by the model using the correct properties, though it is not significant. In the case of modelling conductive heat transfer to the liquid nitrogen pool, the substrate thermal properties should be taken at the liquid nitrogen boiling temperature.

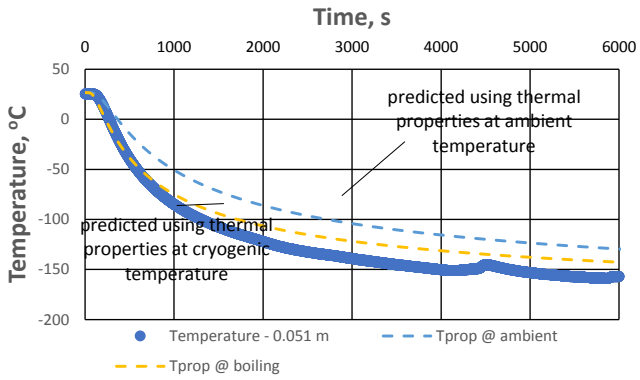

Figure 10: Comparison of 1D model simulation (dotted lines) with measured temperature 5 cm through the concrete

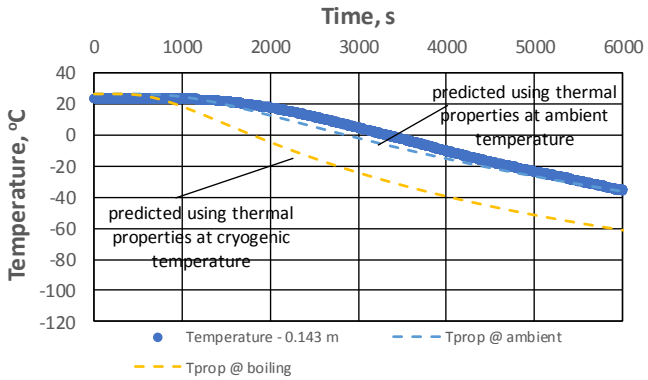

Figure 11: Comparison of 1D model simulation (dotted lines) with measured temperature 15 cm through the concrete

GASP Pool Spreading Model Validation

In this section, Gas Accumulation for Spreading Pools (GASP) was validated with pool spreading data. GASP was assessed with the generated experimental data, as well as available data by Moorhouse and Carpenter (1986) and Nguyen et al. (2015) (**Error! Reference source not found.**, to **Error! Reference source not found.**). The only heat source taken into account in this exercise was conduction from the ground. According to Véchot et al. (2012), the effect of convective heat transfer becomes gradually important to the overall heat transfer to the pool when the spill last long and it can be even 30% of total contribution after 10 min pool duration. However, Moorhouse and Carpenter (1986) pool spreading lasted only 300 s, and the pool spreading generated in this study as well as Nguyen et al. (2015) study lasted only 100 s, which is the period when the conductive heat transfer from the concrete is much higher than other modes of the heat transfer combined.

The input data for model validation against Moorhouse and Carpenter (1986) experiment are displayed in Table 7. LNG was spilled at a rate of 17 tonnes min^{-1} into the apex of a 45° sector, which would be an equivalent of 136 tonnes min^{-1} if the spill was spread in all directions. A validation study of GASP with the data of Moorhouse and Carpenter (1986) have already been done previously by Webber (1991), and it was repeated in this study for verification of the code and as a basis of comparison. The comparisons between the GASP simulations Moorhouse and Carpenter (1986) data are displayed in **Error! Reference source not found.**.

Table 7: GASP input data for continuous release of LNG done by Moorhouse and Carpenter (1986)

Input data from Moorhouse and Carpenter (1986)	
Liquid	Methane
Spill rate, kg s^{-1}	5.16
Spill time, s	300
Density of liquid, kg m^{-3}	460
Initial ground temperature, ° C	20
Additional assumptions	
Initial h/r ratio (shape of cylindrical tank)	1.5
Ground	Smooth concrete
Thermal conductivity, W m^{-1} K^{-1}	1.7
Thermal diffusivity, m^2 s^{-1}	5×10^{-7}
Shape factor	Smooth, 0

GASP was then compared against the pool spreading data generated in this study. Since the base of the concrete pit had a 1% slope towards the SW corner, the way the pool spread was also not uniform. As an intermediate solution, the data for the pool spreading was averaged between one corners to the opposite corners (i.e. NE to SW), resulting in four pool spreading rates. Only the data from Trial 2 of the experiment were used for the pool spreading model validation as the amount of data points in Trial 1 were insufficient. Pool radius was recorded after liquid nitrogen reaches the ground. The input data used for the GASP modelling of the experimental data are shown in **Error! Reference source not found.**.

Table 8: GASP input data for the modelling of experiment at RLESC (Trial 2)

Input data from experiment (Trial 2)	
Liquid	Nitrogen
Spill rate, kg s^{-1}	1.3
Spill time, s	4560
Initial ground temperature, ° C	24.5
Thermal conductivity, W m^{-1} K^{-1}	1.1
Thermal diffusivity, m^2 s^{-1}	5.96×10^{-7}
Additional assumptions	

Initial h/r ratio (shape of cylindrical tank)	1.5
Ground	Smooth concrete
Shape factor	Smooth, 0

Cryogenic pool spreading was investigated by Nguyen et al. (2015) by spilling liquid nitrogen through a funnel onto a concrete plate. The substrate has a radius 0.8 m and thickness 0.025 m. Thermocouples have been aligned in four directions, of 0.05 m apart, starting from the centre of the plate. Liquid is detected where the thermocouples display the liquid nitrogen boiling temperature at -196° C. The container of the plate was rested on a balance with a resolution of 0.1 g. A total of six trials were conducted. Nozzles of dimensions of 6 mm, 8 mm, and 10 mm were used to maintain the spill flowrates at 3.4×10^{-2} kg s^{-1}, 5.6×10^{-2} kg s^{-1} and 9.0×10^{-2} kg s^{-1} respectively, which are much lower spill rates than generated in this study and by Moorhouse and Carpenter (1986). A total of 7.5 L of liquid nitrogen was spilled in each trial.

Table 9: GASP Input data for the continuous release of liquid nitrogen experiment by Nguyen *et al.* (2015)

Input data	**Case 1 and 2**	**Case 3 and 4**	**Case 5 and 6**
Liquid	Liquid Nitrogen		
Spill rate, kg s^{-1}	3.4×10^{-2}	5.6×10^{-2}	9.0×10^{-2}
Duration, s	120	80	60
Liquid	Nitrogen	Nitrogen	Nitrogen
Additional assumptions			
Thermal conductivity*, W m^{-1} K^{-1}	1.7		
Thermal diffusivity*, m^2 s^{-1}	5×10^{-7}		

* : data not given by Nguyen *et al.* (2015) and taken from Moorhouse and Carpenter (1986)

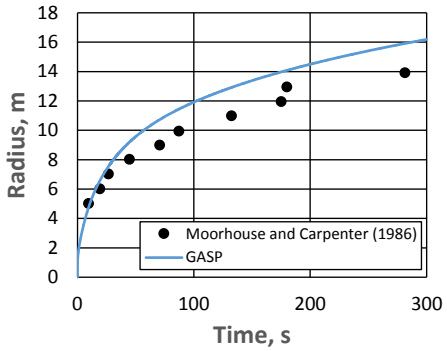

Figure 12: Validation with Moorhouse and Carpenter (1986)

The GASP model simulation for Moorhouse and Carpenter (1986) case is consistent with their experimental data and only slightly over-predicts radius. This simulation matches the simulation done by Webber (1991), with the only difference that the shape factor was taken to be 0 while it was assumed 1 by D. M. Webber. Thus, the simulation can be optimized if the additional parameter was added.

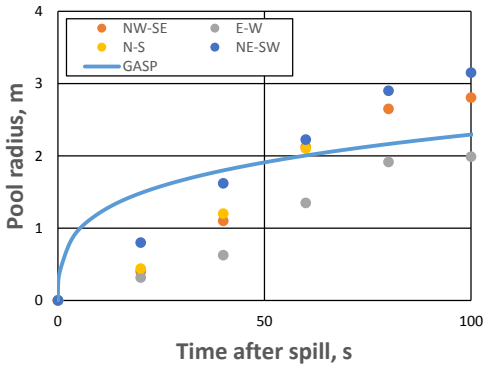

Figure 13: Radius of pool as in all 8 measured directions (Trial 2)

When GASP was set to simulate the experimental data, the predicted radius initially overshoots. GASP then progresses to underestimate the pool at the last half of the spill, as seen in Figure 13. The experimental maximum pool radius varies according

to the side at which side the pool is spreading because of the 1% slope. The simulation does not exhibit a large quantitative difference when compared to the experimental data. It does, however, provides a conservative prediction of the vaporization rate of cryogenic spills and an underestimation of the pool spreading rate for the last 50 s.

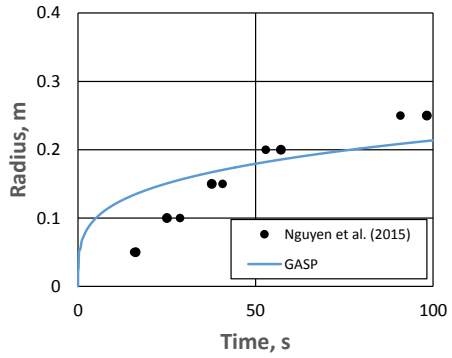

Figure 14: Validation of Model 2 and 3 against pool spreading data (Case 1 and 2)

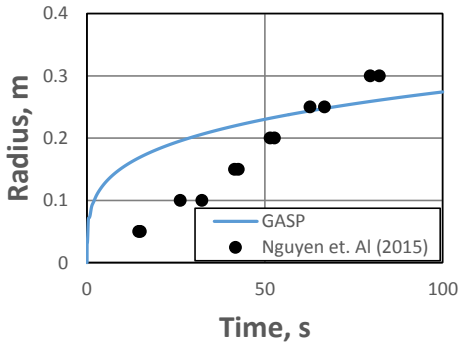

Figure 15: Validation of Model 2 and 3 against pool spreading data (Case 3 and 4)

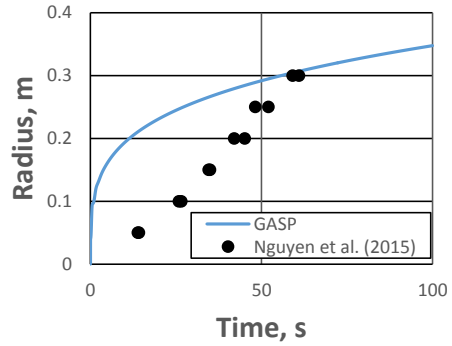

Figure 16: Validation of Model 2 and 3 against pool spreading data (Case 5 and 6)

The performance of GASP when simulating the data by Nguyen et al. (2015) was consistent with its performance when simulating the data generated in this study. The initial high pool growth rate predicted by the model was absent in the experiment. As seen in Figure 14 and Figure 15, GASP initially overestimates the pool radius and then progresses to underpredict it. The lack of data after 50 s in Cases 5 and 6 (Figure 16) prevents us from making the sure conclusions.

When compared to our generated data and the data by Nguyen et al. (2015), the radii predicted by GASP are initially higher for approximately the first half of the spill as the experimental pool initially grew slower than the simulated pool. In contrast to this, the trend of the pool growth observed in Moorhouse and Carpenter (1986)'s experiment correlated with the model throughout the spill. There are two possibilities. It was hypothesized that vaporization may have occurred before the liquid was in contact with concrete (i.e. through flashing at the hose) at the early stages of the spill, which means that less liquid nitrogen was available to form a pool. The reason for flashing may be due to the heat from the sun or wind transmitted through the hose or the funnel, not taken into account inside the model. Eventually, the pool grows faster than the simulation because the source (i.e. hose) cooled down and all of the incoming liquid nitrogen was discharged into the pit. This hypothesis is possible, as the camera installed outside of the pit did show vapour leaving before the liquid.

Another hypothesis is that the model does not simulate well for slow spills. The spill done by Moorhouse and Carpenter (1986) was a magnitude higher than our experiment. While the data provided Moorhouse and Carpenter (1986) starts at 5 m, our experiment ends at 3 m. The third simulation conducted on Nguyen et al. (2015)'s data provides repeatability of the observations for slow spill simulations when using different spill setup and weather conditions.

Both data generated in this experiment and Nguyen *et al.* (2015) show a relatively linear trend between pool radius and time, but it must be noticed these are very short spills. This linear trend has been explained by Webber (1991) to occur when the gravity force acting on the pool is in balance with the pool inertia. In Equation 2, the gravity-inertia regime is represented when the friction term F is still zero or negligible. Figure 17 and Figure 18 display the comparison of the gravity and friction terms during each simulation. It can be observed that the gravity-inertia regime occurs instantaneously inside the model (within less than a millisecond or so), which then causes the linear trend to be negligible in this model, not reflected in our experimental data and the data from Nguyen *et al.* (2015).

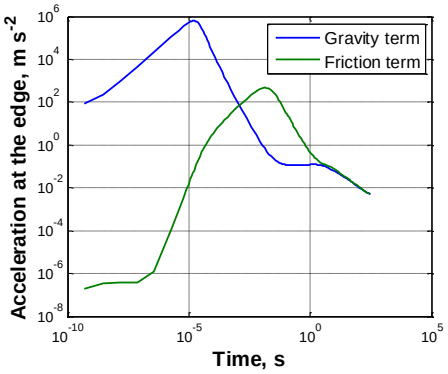

Figure 17: Simulation of the gravity and friction terms for Moorhouse and Carpenter (1986) data

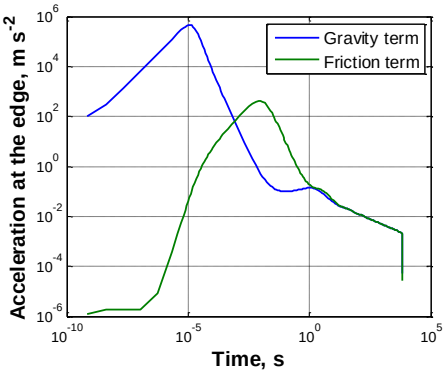

Figure 18: Simulation of the gravity and friction terms for the generated experimental data

Conclusion

The objective of this work is to validate existing source term models of liquefied natural gas (LNG) spills on concrete ground with a new set of experimental data at medium scale. Two spills of liquid nitrogen on a 5 x 6 x 1.2 m pit were done to provide larger scale experimental data for existing cryogenic source term models. In each trial, pool temperature, pool spreading rate, and temperature change within the concrete were measured. Twenty-seven thermocouples have been aligned in 8 directions at the base of the pit to measure pool radius. Under the concrete, thermocouples were arranged to measure temperature under the ground at 0.05 m and 0.15 m depths. The pool front was detected by the measurement of the boiling temperature of liquid nitrogen at the thermocouple. As a result, the pool temperature and temperature of the concrete at 0.05 m and 0.15 m depth below the surface were used to justify the assumptions incorporated inside the model. The model was also directly validated with the experiment through the comparison of pool radius and temperature under the concrete.

The pool radius estimated by GASP was found to be relatively close with the experimental data, although it simulates the experiment by Moorhouse and Carpenter (1986) much better than our experiment. For the simulation of our experimental data, the model and the radius data do not display the same trend. While the experimental data show a linear trend between radius and time, the model displays a curve. There were two hypothesis behind this scenario. The first is that vaporization inside the hose was speculated to decrease the discharge rate of liquid nitrogen onto the ground, causing the pool to spread slower at the beginning of the spill. The second is that the gravity-inertia regime simulated by the model ended too soon for simulations of slow spills. The same observations regarding the linearity of the pool spreading rate was found in Nguyen *et al.* (2015) data for a relatively slow liquid nitrogen spill on concrete. In the future, the modelling of a cryogenic liquid pool should be further examined for slow leakages with rates are equal to or less than the magnitude of 10^{-3} m^3 s^{-1} to conclude which hypothesis is more plausible.

At the base, temperature below the centre of the pool decreased faster than other nodes, implying the effect of spreading upon the total heat transfer. Not taking into account higher heat transfer at the outer rings of the pool would underestimate the total heat transfer from the ground and thus overestimate pool radius and underestimate vaporization rate. Fourier's classic one-dimensional conduction equation solution was able to predict the concrete temperature underground, although with a slight overestimation. The simulation of the concrete temperature was conducted twice, once using the thermal properties of the substrate at ambient temperature and the second using the thermal properties at liquid nitrogen boiling temperature. It was found that the temperature at which the thermal properties were taken does affect the accuracy of the model to the experimental data.

In the case of modelling conductive heat transfer to the liquid nitrogen pool, the substrate thermal properties should be taken at the liquid nitrogen boiling temperature. Overall, Fourier's conduction equation is sufficient to model conductive heat transfer to the pool. It is able to predict the concrete temperature with a maximum of 11.3% overestimation when simulated with the generated liquid nitrogen spill data. Incorporation of the boiling regimes inside the model may be considered for a more realistic simulation of the heat transfer contact between the ground and the liquid pool, however it does not seem crucial.

References

Ahammad, M., Quraishy, S., Olewski, T., Véchot, L., 2017. Small-scale field spill experiments of liquid nitrogen, oxygen and their mixture on concrete surface. J. Loss Prev. Process Ind. 50, 112–120. doi:10.1016/j.jlp.2017.09.009

Hankinson, G., Murphy, D.J., 1987. private communication.

International Gas Union, 2017. 2017 World LNG Report.

Lang, R.Z.J., Moorhouse, J., Paul, G.J., 1980. Waterproof insulation materials, in: Insititution of Chemical Engineers Seventh Symposium on Process Hazards.

Moorhouse, J., Carpenter, R.J., 1986. Factors affecting vapour evolution rates from liquefied gas spills. North West. Branch Pap. Inst. Chem. Eng. 1, 4.1–4.18.

Nguyen, D., Kim, M., Choi, B., Kim, T., 2015. Experimental study of the evaporation of spreading liquid nitrogen, in: The 2015 World Congress on "Advances in Aeronautics, Nano, Bio, Robotics, and Energy (ANBRE15)." Incheon, pp. 68–73. doi:10.1016/j.jlp.2015.11.018

Quraishy, S., Sadia, A., Olewski, T., Véchot, L., 2015. Modelling of Transition and Nucleate Boiling of Liquid Nitrogen Spill on Concrete, in: Hazards 25.

Reid, R.C.C., Wang, R., 1978a. The boiling rates of LNG on typical dike floor materials. Cryogenics (Guildf). 18, 401–404. doi:http://dx.doi.org/10.1016/0011-2275(78)90033-4

Reid, R.C.C., Wang, R., 1978b. The boiling rates of LNG on typical dike floor materials. Cryogenics (Guildf). 18, 401–404. doi:http://dx.doi.org/10.1016/0011-2275(78)90033-4

Véchot, L., Olewski, T., Osorio, C., Basha, O., Liu, Y., Mannan, S., 2012. Laboratory scale analysis of the influence of different heat transfer mechanisms on liquid nitrogen vaporization rate [WWW Document]. J. Loss Prev. Process Ind. doi:10.1016/j.jlp.2012.07.019

Vechot, N.L., Olewski, T., Ulumuddin, N., Quraishy, S., Ghannam, S., Sadia, A., Mannan, S., Ahammad, 2017. Source term modeling of LNG vapor formation by experimental investigation and CFD simulation. Doha.

Webber, D.M., 1991. Source terms. J. Loss Prev. Process Ind. 4, 5–15. doi:10.1016/0950-4230(91)80002-C

Webber, D.M., Brighton, P.W.M., 1987. An integral model for spreading, vaporising pools (No. SRD-R-390; GB_1987:55260), HSE Reports. UKAEA Safety and Reliability Directorate, Warrington.

Webber, D.M., Gant, S.E., Ivings, M.J., Jagger, S.F., 2010. LNG source term models for hazard analysis: A review of the state-of-the-art and an approach to model assessment (No. Research Report: RR789), HSE Books. Buxton, Derbyshire, UK.